Interannual variability of Arctic sea ice export into the East Greenland Current

K. A. Cox,[1] J. D. Stanford,[1] A. J. McVicar,[1,2] E. J. Rohling,[1] K. J. Heywood,[3] S. Bacon,[1] M. Bolshaw,[1] P. A. Dodd,[4] S. De la Rosa,[1,5] and D. Wilkinson[1]

Received 24 February 2010; revised 6 October 2010; accepted 21 October 2010; published 28 December 2010.

[1] Observations since the 1950s suggest that the Arctic climate system is changing in response to rising global air temperatures. These changes include an intensified hydrological cycle, Arctic sea ice decline, and increasing Greenland glacial melt. Here we use new $\delta^{18}O$ data from the East Greenland Current system at Cape Farewell and Denmark Strait to determine the relative proportions of the freshwater components within the East Greenland Current and East Greenland Coastal Current. Through the comparison of these new data with historical studies, we gain insight into the changing Arctic freshwater balance. We detect three key shifts in the net freshwater component $\delta^{18}O$ values, these are (1) a shift to lighter values in the late 1990s that possibly indicates an increased Greenland glacial melt or a reduced sea ice melt admixture and (2) a short-term shift to a ~10‰ heavier value in 2005 followed by (3) a shift back to the historic average value in 2008. The latter fluctuation reflects a short-term dramatic rise and fall of sea ice meltwater addition into the East Greenland Current system. We infer that this anomalously large inclusion of sea ice meltwater resulted from a short-term peak in Arctic sea ice export via Fram Strait. Our findings, therefore, suggest that the freshwater carried in the East Greenland Current system is susceptible to short-term, high-amplitude changes in the upstream freshwater balance, which may have important ramifications for the global thermohaline circulation through the suppression of deep water formation in the North Atlantic.

Citation: Cox, K. A., J. D. Stanford, A. J. McVicar, E. J. Rohling, K. J. Heywood, S. Bacon, M. Bolshaw, P. A. Dodd, S. De la Rosa, and D. Wilkinson (2010), Interannual variability of Arctic sea ice export into the East Greenland Current, *J. Geophys. Res.*, *115*, C12063, doi:10.1029/2010JC006227.

1. Introduction

[2] The Arctic Ocean is the largest oceanic global freshwater reservoir. The key components in the Arctic freshwater balance include: net evaporation and precipitation over the Arctic Ocean; Arctic river run off; the melting and formation of sea ice; Pacific water inflow via Bering Strait; and meltwater from continental ice sheets (specifically the Greenland ice sheet). Freshwater additions into the Arctic basin may be exported to the northern North Atlantic via the Nordic Seas through Fram Strait and via the Canadian Archipelago. Alternatively, freshwater is stored within the Arctic Basin in the form of sea ice or a low-salinity surface water mass above the Arctic halocline [e.g., *Aagaard and Carmack*, 1989].

[3] The East Greenland Current (EGC) and the East Greenland Coastal Current (EGCC) together form the key carriers of freshwater from the Arctic into the northern North Atlantic via Fram Strait. The EGC flows southward out of the Arctic through Fram Strait [*de Steur et al.*, 2009] and along the eastern margin of Greenland via Denmark Strait. As the EGC flows over the wide East Greenland shelf at Denmark Strait, the current crosses the Kangerdlugssuaq Trough, a large canyon that cuts across the shelf (50 m wide and up to 600 m deep, relative to the 250 m deep shelf). The path of the EGC, either entering the canyon with no recirculation, or bifurcating so the main current cuts across the canyon causing an anticyclonic eddy at the head of the canyon [*Sutherland and Cenedese*, 2009]. This may form part of the mechanism for the formation of the EGCC [*Bacon et al.*, 2002, 2008; *Sutherland and Pickart*, 2008; *Sutherland and Cenedese*, 2009]. *Sutherland and Pickart* [2008] suggest that mixing within the canyon would alter the water mass stratification; therefore these changes in bathymetry would promote vertical mixing within the current. In addition, there is strong vertical mixing associated with the East Greenland

[1]National Oceanography Centre, Southampton, School of Ocean and Earth Science, University of Southampton, Southampton, UK.
[2]Department of Earth Science and Engineering and Grantham Institute of Climate Change, Imperial College, London, UK.
[3]School of Environmental Sciences, University of East Anglia, Norwich, UK.
[4]Norsk Polarinstitutt, Polarmiljøsenteret, Tromso, Norway.
[5]Geophysical Institute, University of Bergen, Bergen, Norway.

0148-0227/10/2010JC006227

Table 1. East Greenland Water Mass Salinity and δ^{18}O End-Member Values[a]

Water Mass	Salinity	δ^{18}O (‰)
Arctic meteoric water	0	−21
Greenland glacial meltwater	0	−20 to −40
Sea ice meltwater	3	surface + 2.1
North Atlantic seawater	34.92	0.3

[a]Data from *Bauch et al.* [1995] and *Reeh et al.* [2002].

Spill Jet south of Denmark Strait [*Pickart et al.*, 2005]. At Cape Farewell, the southernmost tip of Greenland, approximately one third of the EGC/EGCC retroflects into the central Irminger Basin [*Holliday et al.*, 2007]. Therefore, the EGC/EGCC forms a direct route for freshwater transport from the Arctic into the subpolar gyre, and consequently into the general ocean circulation of the North Atlantic [*Holliday et al.*, 2007].

[4] The Arctic climate system has undergone major changes since the 1950s as a result of increasing global surface air temperatures [e.g., *Brohan et al.*, 2006]. Specifically, the Arctic sea surface temperatures have increased [*Comiso*, 2003] causing an intensification of the Arctic hydrological cycle [*Solomon et al.*, 2007]. These have been accompanied by net Greenland ice ablation, associated with increased summer surface ice melt and glacier acceleration [e.g., *Krabill et al.*, 2000; *Rignot and Thomas*, 2002; *Rignot and Kanagaratnam*, 2006; *Velicogna*, 2009], a reduction in sea ice extent and thickness [e.g., *Comiso et al.*, 2008; *Kwok et al.*, 2009; *Kwok and Rothrock*, 2009], and Arctic permafrost thawing [e.g., *Osterkamp and Romanovsky*, 1999; *Osterkamp*, 2005].

[5] The Arctic Ocean receives 11% of the global river input through the discharge of major Eurasian and North American rivers [*Shiklomanov et al.*, 2000]. The Eurasian river discharge into the Arctic Ocean has been increasing by ~2 km^3 yr^{-1} yr^{-1} since the 1930s [*Peterson et al.*, 2002; *Wu et al.*, 2005], and between 1964 and 2000 this rate of increase was observed to have more than doubled to 5.6 km^3 yr^{-1} yr^{-1} [*McClelland et al.*, 2006]. This large increase in Eurasian river discharge was only slightly offset by a decrease in the North American river discharge into the Arctic between 1946 and 2000 of −0.4 km^3 yr^{-1} yr^{-1} [*McClelland et al.*, 2006; *Déry and Wood*, 2005]. In addition to this increase in net Arctic river discharge, *New et al.* [2001] reported that precipitation between 60 and 80 °N increased by an average of 0.08% per year, between 1900 and 1998.

[6] Arctic sea ice comprises perennial and seasonal ice. The perennial ice forms the permanent sea ice cover that persists throughout the summer months and, therefore, consists of relatively thick multiyear ice. Conversely, the seasonal sea ice is thinner and melts back every summer. The Arctic perennial sea ice extent has been in decline from at least 1979 when satellite records began [e.g., *Kwok et al.*, 2009]. *Comiso* [2002] and *Stroeve et al.* [2007] report a perennial sea ice extent decline of around 8–10% per decade. However, more recently, the reduction in both sea ice thickness and extent has intensified [*Comiso et al.*, 2008; *Kwok et al.*, 2009; *Kwok and Rothrock*, 2009]. In September 2007 the perennial sea ice cover reached a new extreme minimum such that Canada's Northwest Passage became open to commercial shipping for the first time since observations began 30 years ago [*Comiso et al.*, 2008; *Kwok et al.*, 2009].

[7] The Greenland continental ice sheet is the main source of glacial meltwater to the Arctic Basin and the East Greenland current system. Studies have shown that the Greenland ice sheet has experienced considerable net mass loss since the 1990s [e.g., *Krabill et al.*, 2000; *Rignot and Thomas*, 2002; *Rignot and Kanagaratnam*, 2006; *van den Broeke et al.*, 2009; *Velicogna*, 2009]. The southeastern glaciers are dominated by a negative mass balance that amounts to −17 ± 4 km^3 yr^{-1} [*Rignot et al.*, 2004]. Specifically, the largest East Greenland glaciers, Helheim and Kangerdlugssuaq, were observed to accelerate and retreat abruptly between 2002 and 2005; in 2004 their combined mass loss had doubled [*Luckman et al.*, 2006; *Howat et al.*, 2007]. These rates of ice loss returned to near-previous values in 2006 following reequilibration of the glacier calving fronts [*Howat et al.*, 2007]. *Howat et al.* [2008] concluded that, in part, the rising surface air and sea surface temperatures drove these episodes of glacial acceleration and retreat and, therefore, they may occur more frequently in a warming climate.

[8] The result of these processes has been a freshening of the Arctic Ocean surface water in the Canadian and Makarov basins [*Peterson et al.*, 2006; *McPhee et al.*, 2009, *Yamamoto-Kawai et al.*, 2009]. As these freshened surface waters are exported into the northern North Atlantic, deep water formation in this region may be interrupted and therefore, there may be significant implications for the global thermohaline circulation [e.g., *Stouffer et al.*, 2006]. In this changing climate, it is therefore important to carefully monitor the Arctic freshwater export into the northern North Atlantic.

[9] Here, we present three new salinity and oxygen isotope data sets from water samples collected in the East Greenland region in August–September 2004, 2005, and 2008. We compare these data with historical oxygen isotope studies in this region and, using the new salinity and oxygen isotope ratio data, we characterize the volume and origins of the freshwater end-member components within the EGC and EGCC.

2. Oxygen Isotopes

[10] The freshwater concentration of the EGC and EGCC can be quantified using the salinity anomaly of the EGC/EGCC water relative to a suitable reference salinity [see, e.g., *Wilkinson and Bacon*, 2005]. However, salinity alone cannot distinguish between the different potential origins of the freshwater admixture. This distinction is possible using the stable oxygen isotope ratio (^{18}O/^{16}O) of the EGC/EGCC waters. The ratio of ^{18}O to ^{16}O is expressed as a per mil (‰) deviation from the international Vienna Standard Mean Ocean Water (VSMOW) standard, using the conventional delta notation

$$\delta^{18}O = \left\{ \frac{\left({}^{18}O/{}^{16}O\right)_{sample}}{\left({}^{18}O/{}^{16}O\right)_{VSMOW}} - 1 \right\} \times 1000\ (‰). \tag{1}$$

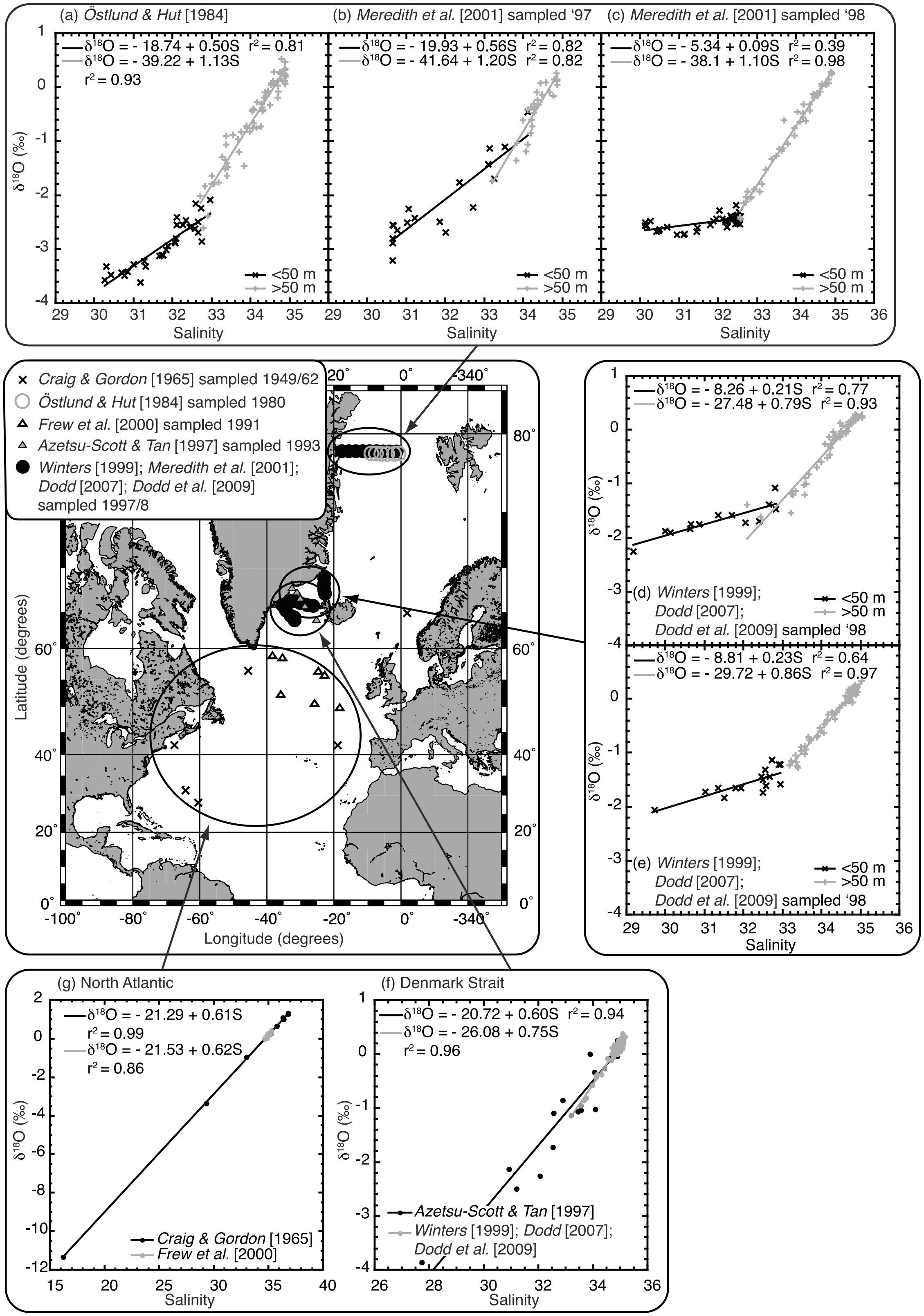

Figure 1. Map of the historic δ^{18}O studies and their corresponding salinity:δ^{18}O mixing relationships. (a–e) The complex two layer mixing relationships and (f and g) the simple mixing relationships are shown. Salinity and δ^{18}O data were retrieved from *Schmidt et al.* [1999].

Table 2. Historic $\delta^{18}O$ Studies and Their Salinity:$\delta^{18}O$ Mixing Relationship Parameters

Locality	Month	Year	Slope	$\delta^{18}O_{NFI}$ (‰)	N	r^2	Reference
Complex Mixing Lines							
Fram Strait	Aug–Sep	1980	0.50	−18.74	31	0.81	*Östlund and Hut* [1984]
Fram Strait	Aug–Sep	1980	1.13	−39.22	68	0.92	*Östlund and Hut* [1984]
Fram Strait	Aug–Sep	1997	0.56	−19.93	18	0.83	*Meredith et al.* [2001]
Fram Strait	Aug–Sep	1997	1.20	−41.64	28	0.81	*Meredith et al.* [2001]
Fram Strait	Aug–Sep	1998	0.09	−5.34	40	0.38	*Meredith et al.* [2001]
Fram Strait	Aug–Sep	1998	1.10	−38.1	44	0.98	*Meredith et al.* [2001]
Denmark Strait (1)	Oct	1998	0.21	−8.26	13	0.77	*Winters* [1999], *Dodd* [2007], and *Dodd et al.* [2009]
Denmark Strait (1)	Oct	1998	0.79	−27.48	58	0.92	*Winters* [1999], *Dodd* [2007], and *Dodd et al.* [2009]
Denmark Strait (2)	Oct	1998	0.23	−8.81	16	0.64	*Winters* [1999], *Dodd* [2007], and *Dodd et al.* [2009]
Denmark Strait (2)	Oct	1998	0.86	−29.72	72	0.98	*Winters* [1999], *Dodd* [2007], and *Dodd et al.* [2009]
Simple Mixing Lines							
North of 30°N North Atlantic	–	1949 1962	0.61	−21.29	9	0.99	*Craig and Gordon* [1965]
North Atlantic subpolar gyre	Aug	1991	0.62	−21.53	21	0.86	*Frew et al.* [2000]
Kangerdlugssuaq Fjord	Sep	1993	0.59	−20.72	26	0.94	*Azetsu-Scott and Tan* [1997]
South of Denmark Strait	Oct	1998	0.75	−26.08	87	0.96	*Winters* [1999], *Dodd* [2007], and *Dodd et al.* [2009]

The $\delta^{18}O$ values of the various water masses carried in the EGC/EGCC are summarized in Table 1 [*Bauch et al.*, 1995; *Reeh et al.*, 2002].

[11] The $\delta^{18}O$ of the freshwater intercept on a salinity:$\delta^{18}O$ plot indicates the mass balanced $\delta^{18}O$ of the net freshwater component within the studied water mass. Several studies have reported sea surface water $\delta^{18}O$ values in the East Greenland and northern North Atlantic region (Table 2 and Figure 1). These data were retrieved from the Goddard Institute of Space Studies (GISS) Global Seawater Oxygen-18 Database [*Schmidt et al.*, 1999], in which the $\delta^{18}O$ values have been adjusted using the deep water data from the GEOSECS data set [*Östlund et al.*, 1987] to allow comparisons between data analyzed using different standards, techniques and mass spectrometers. We acknowledge the existence of data sampled from the EGC/EGCC in 2004 [*Sutherland et al.*, 2009]. However, we do not include these data as they only sample the top 50 m of the water column and are therefore not comparable in character to the data we present here, which span the upper 500 m of the water column. This is because the mixing relationship in the upper 50 m is more sensitive to local ice melt on the East Greenland shelf which may mask the Arctic/upstream freshwater signal contained in the upper 500 m of the water column.

[12] The salinity:$\delta^{18}O$ mixing lines from each of the historic studies are also shown in Figure 1. Three Fram Strait transects (Figures 1a–1c) and two from Denmark Strait (Figures 1d and 1e) display a complex mixing line consisting of two distinct layers [*Schmidt et al.*, 1999] (originally reported by *Östlund and Hut* [1984], *Winters* [1999], *Meredith et al.* [2001], *Dodd* [2007], and *Dodd et al.* [2009]). Note that some of the VEINS Denmark Strait data retrieved from the GISS $\delta^{18}O$ database have not been previously published. As the EGC flows southward out of the Arctic via Fram Strait, the surface water (upper 50 m) remains distinct from the layer below (50–500 m). Within the Greenland Sea, turbulent mixing in the EGC is weak with diapycnal diffusivities (κ) ~ 10^{-5} m^2s^{-1} [*Naveira Garabato et al.*, 2004]. Therefore, we infer that upper ocean mixing is mainly wind driven, and confined to around 50 m depth in the water column, the approximate depth of the Ekman layer. The lower layer (50–500 m) in the water column defines a mixing line between Atlantic water and an Arctic meteoric freshwater end-member. This mixing line has been modified by sea ice formation in the Arctic surface waters, driving the mixing line to the right in salinity:$\delta^{18}O$ space, which results in an apparently light freshwater end-member that is coincidentally similar to Greenland glacial ice $\delta^{18}O$ values. The upper layer defines a mixing line between the shallowest/lowest-salinity water of the lower layer, and a freshwater end-member comprising a mixture of Arctic meteoric water, local sea ice melt and Greenland glacial ice meltwater. This layer is likely maintained by the local meltwater addition and therefore, the slope of this mixing line will vary seasonally according to the ice melt.

[13] A third Denmark Strait data set [*Schmidt et al.*, 1999] (originally reported by *Azetsu-Scott and Tan* [1997]), and data sets from the EGC/EGCC to the south of Denmark Strait and the northern North Atlantic [*Craig and Gordon*, 1965; *Schmidt et al.*, 1999] (originally reported by *Winters* [1999], *Frew et al.* [2000], *Dodd* [2007], and *Dodd et al.* [2009]) show a simpler, one-layer mixing relationship (Figures 1f and 1g). Therefore, there is a clear change in the character of the mixing lines between waters to the north of Denmark Strait and those to the south. We suggest that this reflects the stronger turbulence observed in the EGC/EGCC close to the topography, in the Irminger Basin south of Denmark Strait ($\kappa \sim 10^{-3}$ m^2 s^{-1}) [*Lauderdale et al.*, 2008]. Additionally, topography forced mixing likely occurs as the currents cross the Kangerdlugssuaq Trough [*Pickart et al.*, 2005; *Sutherland and Pickart*, 2008; *Sutherland and Cenedese*, 2009]. As a result, the water masses in the mixed layer penetrate below the pycnocline and therefore, at least the upper 500 m of the water column appears less stratified in and southward of Denmark Strait, forming one distinct mixing line. The proposed evolution of the EGC/EGCC from Fram Strait to Cape Farewell is summarized conceptually in Figure 2. The simple mixing lines recorded south of Denmark Strait consistently show a $\delta^{18}O$ of the net

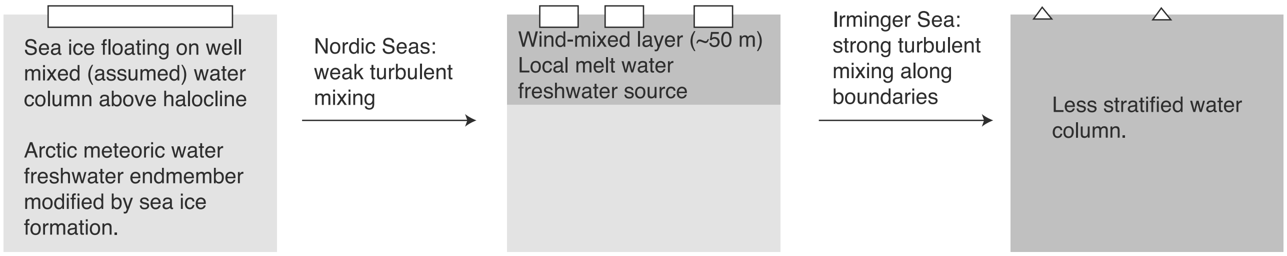

Figure 2. Schematic of the evolution of the upper 500 m of the water column in the EGC/EGCC from Fram Strait to Cape Farewell.

freshwater intercept ($\delta^{18}O_{NFI}$) in the EGC and EGCC, and in the northern North Atlantic, between −20.7‰ and −26.1‰ (Table 2 and Figure 1).

3. Data and Methods

[14] Our water samples were collected on three multidisciplinary oceanographic survey cruises in the East Greenland region. These were the RRS *James Clark Ross* Autosub Under Ice cruise JR106b in Kangerdlugssuaq Fjord and shelf region of East Greenland (Denmark Strait) in August–September 2004 [*Dowdeswell*, 2004], and the RRS *Discovery* cruises D298 [*Bacon*, 2006] and D332 [*Bacon et al.*, 2010] in the East Greenland shelf region at Cape Farewell, South Greenland in August–September 2005 and 2008, respectively (Figure 3). As previously discussed, in this study we focus on the surface water samples collected to a depth of 500 m from the shoreward stations, which comprehensively sample both the EGC and EGCC.

[15] The $\delta^{18}O$ analyses were performed on a GV Instruments Isoprime dual inlet mass spectrometer with Multiprep sample preparation system. Sample aliquots of 0.4 ml were equilibrated with CO_2 gas, and the isotopic difference between the equilibrated CO_2 gas and a reference gas was analyzed. The use of laboratory standards of known composition allows the expression of results in per mil deviations from the international VSMOW standard. All samples were analyzed in duplicate. External precision on the $\delta^{18}O$ analyses is better than 0.05‰ (1σ). Salinity values for the samples were obtained from a Seabird 911 plus CTD mounted on the rosette sampler, calibrated by onboard analysis of discrete samples with a Guildline Autosal 8400B salinometer. External precision of the salinity measurements is better than 0.002 (1σ).

4. Results and Discussion

[16] The salinity:$\delta^{18}O$ mixing relationships defined by the new data are presented in Figure 4. The JR106b (2004) and D332 (2008) salinity:$\delta^{18}O$ mixing lines give a $\delta^{18}O_{NFI}$ of −23.9 ± 1.54‰ (r^2 = 0.98, N = 151) and −22.8 ± 1.48‰ (r^2 = 0.99, N = 114), respectively, in keeping with the historical data. However, the D298 (2005) water data identify an unusually heavy $\delta^{18}O_{NFI}$, relative to the previous studies, with a value of −14.6 ± 1.44‰ (r^2 = 0.99, N = 199). The uncertainty estimates quoted here are the 1σ $\delta^{18}O$ measurement error combined with the 95% confidence interval of the mixing lines.

[17] The $\delta^{18}O_{NFI}$ values recorded in the EGC/EGCC and the northern North Atlantic region since 1965 (Table 2) are plotted in Figure 5. The $\delta^{18}O_{NFI}$ appears to be characterized by three main shifts in the EGC/EGCC region. The observed shifts in the EGC and EGCC waters are indicative of changes in the freshwater budget of these currents, originating either in the Arctic or en route from the Arctic Basin to Cape Farewell. We infer that these shifts in the $\delta^{18}O_{NFI}$ were driven by a compositional change in the low-salinity end of the mixing line, given that all the mixing lines intersect at a point close to the high-salinity Atlantic water end-member (see Table 1 and Figure 4). Consequently, we focus on mechanisms of change in the low-salinity end of

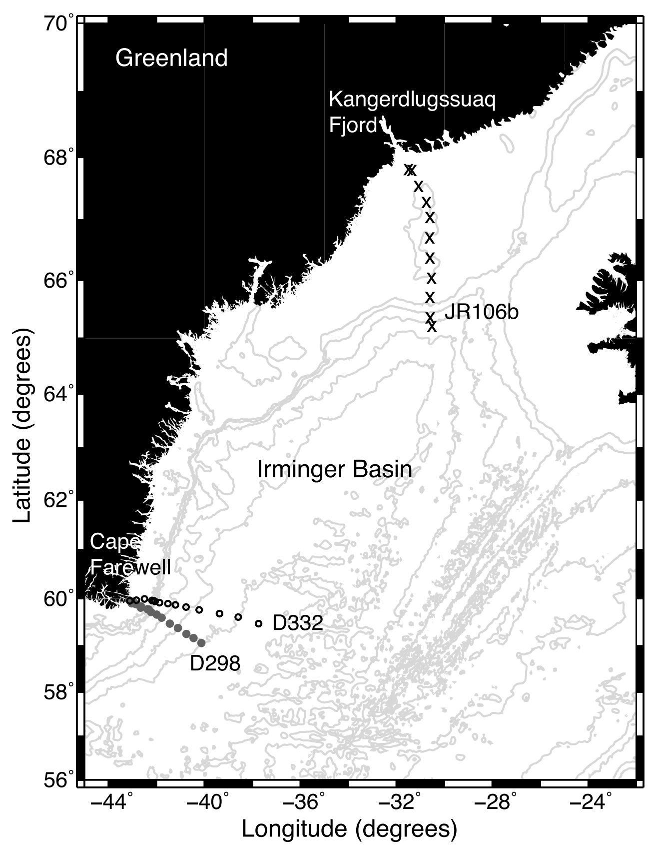

Figure 3. Map of sample locations for the 2004 JR106b data set (crosses), the 2005 D298 data set (solid circles), and the 2008 D332 data set (open circles).

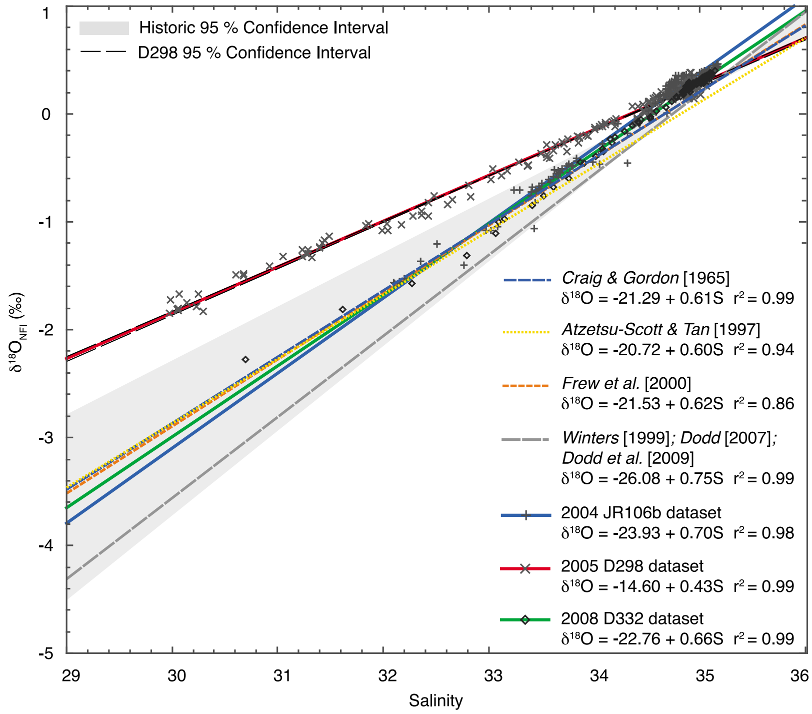

Figure 4. Salinity:δ^{18}O mixing relationships defined by the 2004 JR106b, 2005 D298, and 2008 D332 data compared to the historic simple mixing relationships in the EGC/EGCC and northern North Atlantic region. The 95% confidence intervals are shown for the 2005 D298 data set and the upper and lower limit of the historic data sets.

the mixing line to explain the observed changes in the EGC/EGCC $\delta^{18}O_{NFI}$.

[18] The first shift in the EGC/EGCC $\delta^{18}O_{NFI}$ shown in Figure 5 occurs between 1993 and 1998 in the Kangerdlugssuaq Fjord region in Denmark Strait, with a magnitude of ~5‰ toward a relatively light value. The addition of extra Greenland glacial melt is a possible cause of this shift as it would drive the freshwater end-member to lighter values since the meltwater has isotopic values of −20‰ to −40‰ [*Reeh et al.*, 2002]. Additionally, a reduction in sea ice melt, locally or out of the Arctic, could cause the $\delta^{18}O_{NFI}$ shift to a lighter value. The δ^{18}O fractionation during sea ice formation is relatively small, 2.6‰ [*Macdonald et al.*, 1995], and therefore the δ^{18}O value of sea ice is similar to the Arctic surface water and sea ice meltwater forms a low-salinity water mass that is isotopically relatively heavy with respect to the Arctic river runoff and continental ice (Table 1).

[19] The second shift in the $\delta^{18}O_{NFI}$ indicates that between 2004 and 2005, the freshwater fraction of the EGC/EGCC at Cape Farewell has undergone a seemingly unprecedented change (+~10‰) to an anomalously heavy value (see Figure 5). It is unlikely that this change occurred in the EGC/EGCC en route from Denmark Strait (the location of the 2004 data) to Cape Farewell via Greenland glacial meltwater addition or net precipitation minus evaporation. Freshwater from calving/melting Greenland glacier ice, δ^{18}O of −20‰ or lighter [*Reeh et al.*, 2002], is isotopically too light to have caused the positive shift in $\delta^{18}O_{NFI}$. Similarly, precipitation and runoff over the central to southern regions of East Greenland are not isotopically heavy enough with δ^{18}O values between −10 and −20‰ [*Craig and Gordon*, 1965; *Rozanski et al.*, 1993] and evaporation in this region is insignificant in amount relative to Arctic river runoff and ice melt contributions. Additionally, we have already deduced that these variations in the $\delta^{18}O_{NFI}$ occurred as a result of changes in the freshwater balance, therefore water mass additions from the Irminger Basin with North Atlantic salinity values are unlikely to have caused these changes in $\delta^{18}O_{NFI}$. Consequently, we infer that the Denmark Strait data and the Cape Farewell data are comparable.

[20] Arctic river runoff, δ^{18}O of about −21‰ [*Östlund and Hut*, 1984; *Bauch et al.*, 1995, 2005], is isotopically too light to have caused the positive shift in $\delta^{18}O_{NFI}$. Pacific water addition into the Arctic via Bering Strait has salinity and δ^{18}O values of 33 and −1.0‰, respectively [*Bauch et al.*, 1995], and therefore falls on the mixing line between Atlantic water and Arctic meteoric water so an addition or lack of Pacific water in the EGC/EGCC cannot have caused the relatively heavy EGC/EGCC $\delta^{18}O_{NFI}$ in 2005.

[21] Sea ice meltwater provides a source of isotopically heavy freshwater to the EGC/EGCC (Table 1). We therefore suggest that an increased admixture of sea ice meltwater into the EGC/EGCC is the most viable mechanism for causing a shift in $\delta^{18}O_{NFI}$ of the EGC/EGCC to a heavier value. In summer, all (or most) of the solid Arctic sea ice export via Fram Strait is melted into the EGC/EGCC north of Denmark Strait. Therefore, the extra sea ice meltwater addition to the EGC/EGCC is likely to have occurred upstream of Denmark Strait [*Comiso*, 2002; *Comiso et al.*, 2008]. This sea ice melt

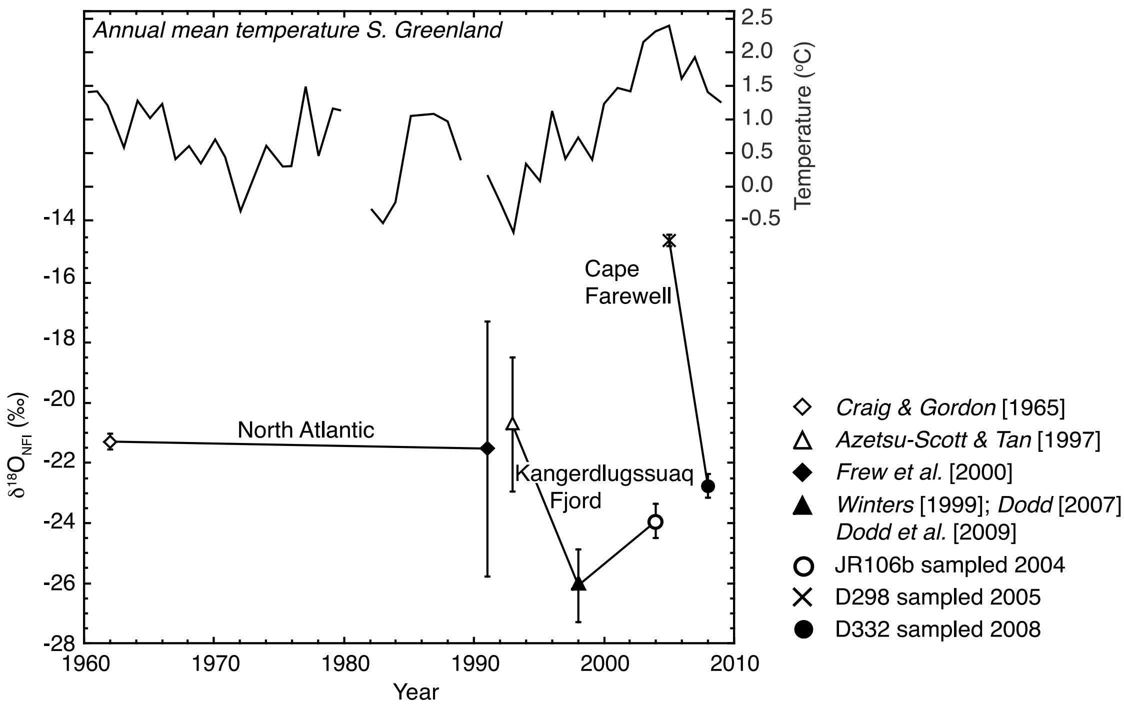

Figure 5. The evolution of the $\delta^{18}O_{NFI}$ in the northern North Atlantic and EGC/EGCC region with time against the annual mean temperature record observed at Prins Christian Sund, South Greenland (60.0°N, 43.2°W). Temperature data were retrieved from the GISS surface temperature analysis (http://data.giss.nasa.gov/gistemp/station_data/) and the $\delta^{18}O_{NFI}$ error bars denote 95% confidence intervals for these values.

signal in the EGC/EGCC coincides with the warmest year on record in Greenland (2005, see Figure 5). The third $\delta^{18}O_{NFI}$ shift, back to a value consistent with the historic average, occurs between 2005 and 2008. This indicates that the increase in sea ice meltwater addition into the EGC/EGCC was a relatively short-term event rather than a longer-term change in the sea ice meltwater export from the Arctic.

[22] We calculate the fractions of meteoric water and sea ice meltwater along the three new EGC/EGCC transects presented in this paper following the end-member mass balance calculation method established by *Bauch et al.* [1995] and *Meredith et al.* [2001]

$$f_{mw} + f_{si} + f_{aw} = 1, \quad (2)$$

$$f_{mw}S_{mw} + f_{si}S_{si} + f_{aw}S_{aw} = S, \quad (3)$$

$$f_{mw}\delta_{mw} + f_{si}\delta_{si} + f_{aw}\delta_{aw} = \delta, \quad (4)$$

where letters *f*, *S* and δ stand for the fraction, salinity, and $\delta^{18}O$, respectively, with the subscripts *mw*, *si*, and *aw* denoting meteoric water (runoff into the Arctic Basin as well as Greenland runoff), sea ice meltwater, and Atlantic water, respectively. The salinity and $\delta^{18}O$ values of the end-members are detailed in Table 1 after those used by *Bauch et al.* [1995] (also used by, for example, *Meredith et al.* [2001] and *Dodd et al.* [2009]). Here, the Greenland glacial meltwater is included within the Arctic meteoric water, which is not strictly valid as these water masses have distinct $\delta^{18}O$ values. However, to discern Greenland glacial meltwater from Arctic meteoric water a third hydrographic tracer is required. In the absence of this, the *Bauch et al.* [1995] end-member values are used to maintain continuity and allow direct comparisons between the studies.

[23] First, we use a meteoric $\delta^{18}O$ (δ_{mw}) value of −21‰ [*Bauch et al.*, 1995]. Then we consider the influence of a lighter value at −35‰, to simulate a mainly glacial origin meteoric end-member. Therefore, we test the sensitivity of the calculation to variations in Greenland glacier meltwater input to the EGC/EGCC. The calculated freshwater concentration sections using a δ_{mw} value of −21‰ are shown in Figures 6a–6f. The meteoric water distributions in the D298 and D332 sections at Cape Farewell (Figures 6c and 6e) are very similar to each other, with the highest meteoric water concentrations at the surface and nearest the Greenland coast, reducing to zero around 50 km from the coast. In the 2004 JR106b section at Kangerdlugssuaq Fjord (Figure 6a), the meteoric water reaches further along the shelf (250 km from Greenland Coast) at the surface and the column inventories (vertical freshwater integration above 150 dbar) indicate that the meteoric water thicknesses in this section are greater, by around 2 m, than in the other two sections. The sea ice meltwater distributions are similar in the 2004 JR106b and 2008 D332 sections with near zero negative fractions across the whole section (Figures 6b and 6f), which indicate net sea ice formation in water masses upstream of these sections. The 2005 D298 section shows a large increase in sea ice melt thickness in the surface 100 m

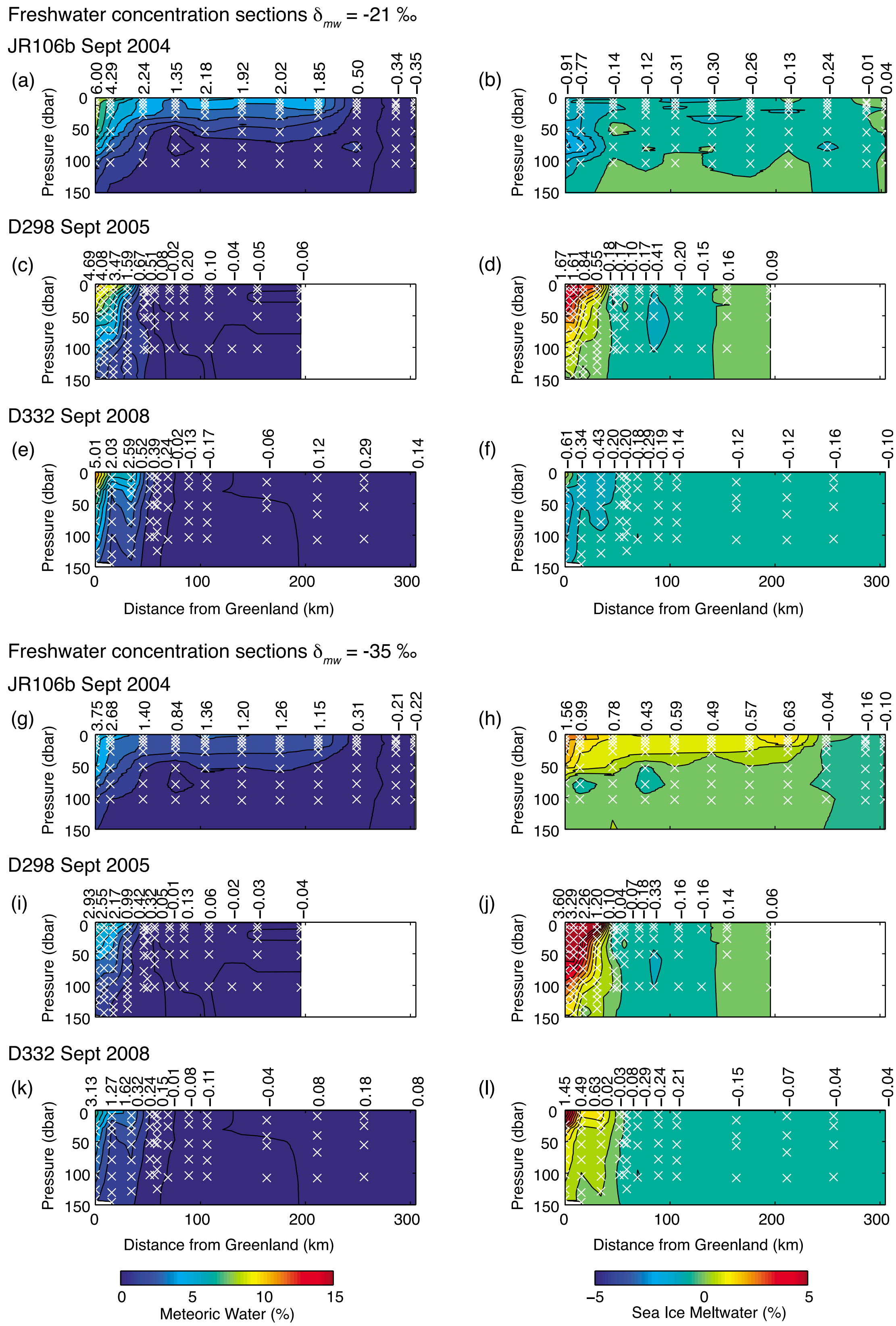

Figure 6. (a–f) Meteoric and sea ice meltwater concentration sections across the EGC/EGCC, calculated using a δ_{mw} value of −21‰, from the 2004 JR106b, 2005 D298, and 2008 D332 data sets. (g–l) As in Figures 6a–6f, however, these were calculated using an extreme light δ_{mw} value of −35‰. The white crosses denote sampling locations and the numbers on top are the column inventories (in m) above 150 dbar.

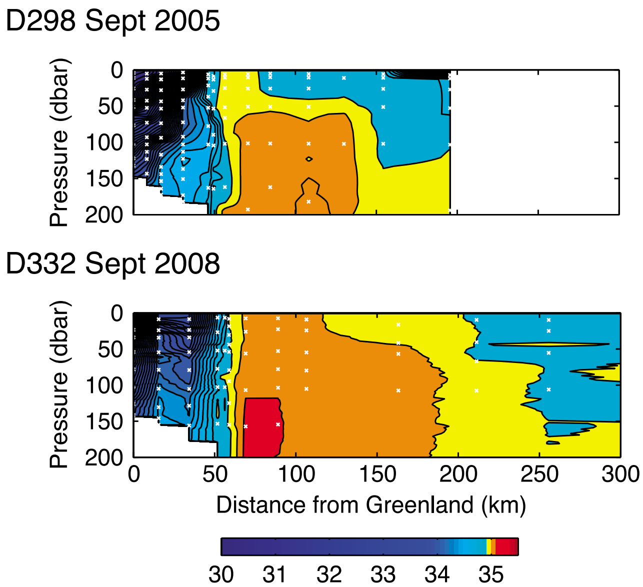

Figure 7. The salinity distribution across the 2005 D298 and 2008 D332 transects, the white crosses denote sampling locations.

within 40 km of the Greenland coast (Figure 6d). This confirms our suggestion that the unusually heavy $\delta^{18}O_{NFI}$ observed in 2005 was a result of an increase in sea ice meltwater admixture to the EGC/EGCC. The positive sea ice melt signal in the 2005 D298 section extends down to the full depth of the shelf (150 m) near the coast, suggesting that this sea ice melt was an Arctic/upstream signal rather than a local ice melt signal.

[24] The freshwater concentration sections using the extreme light δ_{mw} value of −35‰ are shown in Figures 6g–6l. These show that using an extreme light value for the meteoric end-member does not influence the distribution of the freshwater, but the relative concentrations have changed. The sea ice meltwater fraction is nearly doubled and the meteoric water fraction is nearly halved. In each of the sections there is around 2 m less meteoric/glacial meltwater and around 2 m more sea ice meltwater than in the sections calculated using a δ_{mw} of −21‰. However, there is still around 2 m more sea ice melt in the 2005 section relative to the other sections. Therefore, the differences between using a δ_{mw} of −21 and −35‰ in the mass balance calculations do not influence our conclusion that there was an increased sea ice meltwater admixture to the EGC/EGCC in 2005 relative to the other years sampled.

[25] The sea ice meltwater column inventories in Fram Strait reported by *Meredith et al.* [2001] and *Rabe et al.* [2009] range from around −5 to −8 m near the coast (note that negative sea ice melt equates to net sea ice formation). Therefore, our near-zero column inventories observed in the 2004 JR106b and 2008 D332 sections (Figures 6b and 6f) indicate that the melting of sea ice between Fram Strait and Denmark Strait inputs a quantity of freshwater of ~5–8 m during years of more "normal" sea ice meltwater fraction, nearly balancing the observed deficit at Fram Strait. This is comparable to the meteoric water column inventories (4–6 m; Figures 6a and 6e), and demonstrates that the freshwater end-member of the EGCC during "normal years" is composed of roughly equal amounts of meteoric water and sea ice meltwater. This corroborates the idea presented by *Bacon et al.* [2008], that the meltwater from the Fram Strait solid sea ice export has a substantial role in the formation of the EGCC.

[26] Salinity distributions across the 2005 D298 and 2008 D332 transects are shown in Figure 7. These indicate that both transects have a similar salinity distribution, with a freshwater wedge over the East Greenland Shelf where the EGCC is located. The EGC is located just off the shelf with a relatively low-salinity surface water cap over a warm and salty water mass (recirculating Atlantic water). The 2005 D298 transect appears to be more fresh than the 2008 D332 transect, this corroborates our conclusion of a greater ice melt admixture into the EGC/EGCC in 2005.

5. Fram Strait Sea Ice Export

[27] Using a simple mass balance calculation (see Appendix A), we determine the additional sea ice meltwater flux within the EGC/EGCC necessary to shift the $\delta^{18}O_{NFI}$ from the values seen in 2004 and 2008 to the unusually heavy value observed in 2005. We calculate an extra sea ice admixture equal to ~40% of the EGC/EGCC freshwater flux. This represents a mean flux of 99 ± 12 km^3 month^{-1} (see Appendix A).

[28] *Spreen et al.* [2009] reported winter monthly Fram Strait sea ice volume export (2003–2008) from satellite data. Their data do not show any significant long-term trend in Fram Strait sea ice export, but the December 2004 and January 2005 export volumes are exceptionally high relative to the rest of the data, and the December 2004 volume export is nearly double the mean volume export for December 2003/2008 (Table 3). The high sea ice export anomaly of about 100 km^3 month^{-1} in January 2005 [*Spreen et al.*, 2009] is of a similar magnitude to the additional sea ice admixture into the EGC/EGCC required to shift the $\delta^{18}O_{NFI}$ from the 2004 and 2008 values to the anomalously heavy 2005 value (see above; Figure 5). Therefore, allowing 6–7 months transit time from Fram Strait to Cape Farewell, it appears that interannual large amplitude variability in Fram Strait sea ice export has a distinct impact on the freshwater signal observed downstream at Cape Farewell.

[29] The $\delta^{18}O_{NFI}$ in the EGC/EGCC was previously thought to be constant at ~−21‰. However, the EGC/EGCC $\delta^{18}O_{NFI}$ timeline presented here reveals that the freshwater $\delta^{18}O$ signal in this region varies on an interannual timescale, which is related to short-term (interannual), high-amplitude variations in freshwater export from the

Table 3. Fram Strait Monthly Sea Ice Export Data From *Spreen et al.* [2009]

Year	Month	Fram Strait Sea Ice Export (km^3 month^{-1})
2003	Dec	225
2004	Jan	221
2004	Dec	420
2005	Jan	326
2007	Dec	214
2008	Jan	234

Table A1. Parameters Used in Equations (A1)–(A3)

Parameter	Symbol	Value	1σ Uncertainty	Units	Source
$\delta^{18}O_{NFI}$ 2005	δ_{2005}	−14.60	±0.18	‰	This study
$\delta^{18}O_{NFI}$ 2004 and 2008	$\delta_{04/08}$	−23.93 to −22.76	±0.6 and ±0.4	‰	This study
$\delta^{18}O$ of sea ice contribution	δ_{si}	−0.42	±1.0	‰	This study
EGCC/EGC freshwater flux	F_{fw}	0.093×10^6	$\pm 0.0093 \times 10^{6}$[a]	$m^3\ s^{-1}$	[b]
Sea ice extent	x_{si}	7.04×10^{12}	$\pm 0.55 \times 10^{12}$	m^2	*Stroeve et al.* [2005]
Sea ice thickness	z_{si}	2.73	±0.27[a]	m	*Laxon et al.* [2003] and *Thomas et al.* [1996]
Snow thickness	z_{snow}	0.34	±0.03[a]	m	*Warren et al.* [1999]
Sea ice density	ρ_{si}	915.1	–	$kg\ m^{-3}$	*Perovich et al.* [1998]
Snow density	ρ_{snow}	300	–	$kg\ m^{-3}$	*Warren et al.* [1999]
Seawater density	ρ_{sw}	1023.9	–	$kg\ m^{-3}$	–

[a]No reported uncertainties were found, subsequently a 10% uncertainty on the value was assumed in the absence of a 1σ uncertainty.
[b]This value is a combination of the freshwater fluxes of both the EGCC and the EGC. The estimated EGCC freshwater flux is $0.06 \times 10^6\ m^3\ s^{-1}$, based on measurements made in 1997 [*Bacon et al.*, 2002]. An EGC freshwater flux of $0.096 \times 10^6\ m^3\ s^{-1}$ was estimated using an estimated total transport of $4 \times 10^6\ m^3\ s^{-1}$ [*Schlichtholz and Houssais*, 1999] and a long-term mean EGC salinity of 34.67 [*Hughes and Lavin*, 2005] relative to a reference salinity of 34.956 [*Bacon et al.*, 2002; *Wilkinson and Bacon*, 2005].

Arctic through Fram Strait. The transfer of these variations in the Fram Strait freshwater export downstream to Cape Farewell means that these freshwater signals can potentially reach areas of deep water formation.

6. Conclusions

[30] Mass balance calculations using salinity and $\delta^{18}O$ are a useful tool for identifying the freshwater composition of water masses. Comparison of freshwater column inventories defined by our data at Denmark Strait and Cape Farewell with those from Fram Strait [*Meredith et al.*, 2001] has highlighted the important role of sea ice meltwater in the formation of the EGCC. Additionally, we have found that the $\delta^{18}O_{NFI}$ of the EGC/EGCC region and the northern North Atlantic is not constant through the ~60 year oxygen isotope record. Three key shifts have occurred in the $\delta^{18}O_{NFI}$ in this region. We ascribe the first, of ~5‰ at Kangerdlugssuaq Fjord in Denmark Strait to a relatively light value between 1993 and 1998, either to an increased Greenland glacial meltwater admixture into the EGC/EGCC [*Luckman et al.*, 2006; *Howat et al.*, 2007] or a lack of sea ice melt addition to the currents. We calculate that the second $\delta^{18}O_{NFI}$ shift, to an ~10‰ heavier value between 2004 and 2005, at Cape Farewell, reflects an increased admixture of sea ice meltwater into the EGC/EGCC (equal to ~40% of the total freshwater flux) in 2005 relative to the other years sampled. It appears that this large, short-term increase in the sea ice meltwater addition is directly related to a peak in sea ice export via Fram Strait in December 2004 and January 2005 [*Spreen et al.*, 2009]. This reveals that the EGC/EGCC $\delta^{18}O_{NFI}$ is sensitive to short-term (interannual), high-amplitude variations in freshwater export from the Arctic through Fram Strait. The third EGC/EGCC $\delta^{18}O_{NFI}$ shift in the period 2005–2008, back to a value consistent with historic values, highlights the interannual nature of variability in the Arctic export freshwater $\delta^{18}O$ signal, which was previously thought to be constant at ~−21‰. Increases in freshwater flux into the northern North Atlantic may have ramifications for the global thermohaline circulation and it is therefore important to link short- and long-term variations in the freshwater flux through Fram Strait (both solid and liquid) to the downstream freshwater flux at Cape Farewell, where part of the current retroflects directly into the North Atlantic subpolar gyre [*Holliday et al.*, 2007].

Appendix A: Mass Balance Calculation

[31] Here we use a simple mass balance calculation to determine the additional sea ice admixture to the EGC/EGCC required to shift the $\delta^{18}O_{NFI}$ to the anomalously heavy value observed in August–September 2005, using the D298 $\delta^{18}O_{NFI}$ of −14.60‰ relative to the JR106b (2004) and D332 (2008) $\delta^{18}O_{NFI}$ of −23.93 and −22.76‰.

[32] Arctic multiyear sea ice on average comprises 96% by volume of sea ice, and 4% by volume of snow, calculated using equations (A1) and (A2)

$$\%_{ice} = \frac{x_{si} z_{si} \frac{\rho_{si}}{\rho_{sw}}}{x_{si} z_{si} \frac{\rho_{si}}{\rho_{sw}} + x_{si} z_{snow} \frac{\rho_{snow}}{\rho_{sw}}}, \tag{A1}$$

$$\%_{snow} = \frac{x_{si} z_{snow} \frac{\rho_{snow}}{\rho_{sw}}}{x_{si} z_{si} \frac{\rho_{si}}{\rho_{sw}} + x_{si} z_{snow} \frac{\rho_{snow}}{\rho_{sw}}}, \tag{A2}$$

where $\%_{ice}$ and $\%_{snow}$ are the percentages of ice and snow comprising sea ice. The other parameters are summarized in Table A1.

[33] Multiyear sea ice has a salinity of around 4 [*Östlund and Hut*, 1984]. The fractionation of $\delta^{18}O$ during sea ice formation is 2.6‰ [*Macdonald et al.*, 1995], and the $\delta^{18}O$ of Arctic surface seawater is around −3.3 to −1.3‰ [*Yamamoto-Kawai et al.*, 2005]. Therefore, the $\delta^{18}O$ of sea ice ranges from −0.8 to 1.4‰, and we use a mean value of 0.3‰ in accordance with *Yamamoto-Kawai et al.* [2005].

[34] The salinity and $\delta^{18}O$ of the snow covering multiyear sea ice are typically 0 and −18‰, respectively [*Yamamoto-Kawai et al.*, 2005]. Using these values for salinity and $\delta^{18}O$ of multiyear sea ice and its snow load in combination with the above percentages of snow and sea ice constituting multiyear sea ice, the mass balanced salinity and $\delta^{18}O$ effect of the freshwater flux from multiyear sea ice melt (with snow) can be determined as 3.84 and −0.42‰, respectively.

[35] Using the salinity and δ^{18}O effect of sea ice and the $\delta^{18}O_{NFI}$ values of the JR106b (2004) and D332 (2008) data sets compared to the $\delta^{18}O_{NFI}$ of the D298 (2005) data set, we calculate the percentage of sea ice meltwater entering the EGC/EGCC at Fram Strait necessary to cause the 2005 $\delta^{18}O_{NFI}$ shift relative to the 2004 and 2008 $\delta^{18}O_{NFI}$. Using a simple mass balance between the $\delta^{18}O_{NFI}$ values the contribution of extra sea ice melt is 37–44% of the EGC/EGCC freshwater flux.

[36] Next, we determine the flux of this extra sea ice melt admixture using

$$F_{si} = \%_{si} \times F_{fw}, \tag{A3}$$

where F_{si} is the flux of extra sea ice within the EGC/EGCC necessary to cause the relatively heavy $\delta^{18}O_{NFI}$ in the 2005 D298 samples. This yields values of 102.5 ± 11.87 and 94.7 ± 11.87 km^3 $month^{-1}$ relative to the JR106b 2004 and D332 2008 $\delta^{18}O_{NFI}$ values, respectively. The parameters and their uncertainly estimates used in this calculation are summarized in Table A1.

[37] **Acknowledgments.** We thank the entire crew and science parties of the RRS *James Clark Ross* cruise JR106b and the RRS *Discovery* cruises D298 and D332 for their assistance and support during sampling. This project was supported by the Natural Environment Research Council's RAPID climate change and Autosub Under Ice thematic programs. The data presented in this paper have been submitted to the BODC (http://www.bodc.ac.uk) and GISS (http://data.giss.nasa.gov/o18data/) databases.

References

Aagaard, K., and E. C. Carmack (1989), The role of sea ice and other fresh water in the Arctic Circulation, *J. Geophys. Res.*, *94*, 14,485–14,498, doi:10.1029/JC094iC10p14485.

Azetsu-Scott, K., and F. C. Tan (1997), Oxygen isotope studies from Iceland to an East Greenland Fjord: Behavior of glacial meltwater plume, *Mar. Chem.*, *56*, 239–251, doi:10.1016/S0304-4203(96)00078-3.

Bacon, S. (2006), RRS *Discovery* Cruise 298, 23 Aug-25 Sep 2005. Cape Farewell and Eirik Ridge (CFER-1), *Southampton Cruise Rep. 10*, 113 pp., Natl. Oceanogr. Cent., Southampton, U. K.

Bacon, S., G. Reverdin, I. G. Rigor, and H. M. Snaith (2002), A freshwater jet on the east Greenland shelf, *J. Geophys. Res.*, *107*(C7), 3068, doi:10.1029/2001JC000935.

Bacon, S., P. Myers, B. Rudels, and D. Sutherland (2008), Accessing the Inaccessible: Buoyancy-driven coastal currents on the shelves of Greenland and eastern Canada, in *Arctic-Subarctic Ocean Fluxes: Defining the role of the Northern Seas in Climate*, edited by R. R. Dickson, J. Meincke, and P. Rhines, pp. 701–720, Springer-Verlag, Berlin.

Bacon, S., et al. (2010), RRS *Discovery* Cruise 332, 21 Aug-25 Sep 2010. Arctic Gateway (WOCE AR7), *Southampton Cruise Rep. 53*, 129 pp., Natl. Oceanogr. Cent., Southampton, U. K.

Bauch, D., P. Schlosser, and R. G. Fairbanks (1995), Freshwater balance and the sources of deep and bottom waters in the Arctic Ocean inferred from the distribution of $H_2^{18}O$, *Prog. Oceanogr.*, *35*, 53–80, doi:10.1016/0079-6611(95)00005-2.

Bauch, D., H. Erlenkeuser, and N. Andersen (2005), Water mass processes on Arctic shelves as revealed from δ^{18}O of H_2O, *Global Planet. Change*, *48*, 165–174, doi:10.1016/j.gloplacha.2004.12.011.

Brohan, P., J. J. Kennedy, I. Harris, S. F. B. Tett, and P. D. Jones (2006), Uncertainty estimates in regional and global observed temperature changes: A new data set from 1850, *J. Geophys. Res.*, *111*, D12106, doi:10.1029/2005JD006548.

Comiso, J. C. (2002), A rapidly declining perennial sea ice cover in the Arctic, *Geophys. Res. Lett.*, *29*(20), 1956, doi:10.1029/2002GL015650.

Comiso, J. C. (2003), Warming trends in the Arctic from clear sky satellite observations, *J. Clim.*, *16*, 3498–3510, doi:10.1175/1520-0442(2003)016<3498:WTITAF>2.0.CO;2.

Comiso, J. C., C. L. Parkinson, R. Gersten, and L. Stock (2008), Accelerated decline in the Arctic Sea ice cover, *Geophys. Res. Lett.*, *35*, L01703, doi:10.1029/2007GL031972.

Craig, H., and L. I. Gordon (1965), Deuterium and oxygen 18 variations in the ocean and the marine atmosphere in stable isotopes, in *Oceanographic Studies and Paleotemperatures*, edited by E. Tongiori, pp. 9–130, Cons. Naz. delle Ric., Spolento, Italy.

Déry, S. J., and E. F. Wood (2005), Decreasing river discharge in northern Canada, *Geophys. Res. Lett.*, *32*, L10401, doi:10.1029/2005GL022845.

de Steur, L., E. Hansen, R. Gerdes, M. Karcher, E. Fahrbach, and J. Holfort (2009), Freshwater fluxes in the East Greenland Current: A decade of observations, *Geophys. Res. Lett.*, *36*, L23611, doi:10.1029/2009GL041278.

Dodd, P. A. (2007), Freshwater transport in the East Greenland Current, Ph.D. thesis, Sch. of Environ. Sci., Univ. of East Anglia, Norwich, U. K.

Dodd, P. A., K. J. Heywood, M. P. Meredith, A. C. Naveira-Garabato, A. D. Marca, and K. K. Falkner (2009), Sources and fate of freshwater exported in the East Greenland Current, *Geophys. Res. Lett.*, *36*, L19608, doi:10.1029/2009GL039663.

Dowdeswell, J. (2004), RRS *James Clark Ross* Cruise 106b, 30 Aug-16 Sep 2005 NERC Autosub Under Ice Thematic Programme Kangerdlussuaq Fjord and East Greenland Shelf, report, 97 pp., Scott Polar Res. Inst., Univ. of Cambridge, Cambridge, U. K.

Frew, R. D., P. F. Dennis, K. J. Heywood, M. P. Meredith, and S. M. Boswell (2000), The oxygen isotope composition of water masses in the northern North Atlantic, *Deep Sea Res. Part I*, *47*, 2265–2286, doi:10.1016/S0967-0637(00)00023-6.

Holliday, N. P., A. Meyer, S. Bacon, S. G. Alderson, and B. de Cuevas (2007), Retroflection of part of the East Greenland Current at Cape Farewell, *Geophys. Res. Lett.*, *34*, L07609, doi:10.1029/2006GL029085.

Howat, I. M., I. Joughin, and T. A. Scambos (2007), Rapid changes in ice discharge from Greenland outlet glaciers, *Science*, *315*, 1559–1561, doi:10.1126/science.1138478.

Howat, I. M., I. Joughin, M. Fahnestock, B. E. Smith, and T. A. Scambos (2008), Synchronous retreat and acceleration of southeast Greenland outlet glaciers 2000–06: Ice dynamics and coupling to climate, *J. Glaciol.*, *54*, 646–660, doi:10.3189/002214308786570908.

Hughes, S. L., and A. Lavin (2005), ICES report on ocean climate 2005, *ICES Coop. Res. Rep. 280*, Int. Counc. for the Explor. of the Sea, Copenhagen. (Available at http://www.noc.soton.ac.uk/ooc/ICES_WGOH/iroc.php.)

Krabill, W., W. Abdalati, E. Frederick, S. Manizade, C. Martin, J. Sonntag, R. Swift, R. Thomas, W. Wright, and J. Yungel (2000), Greenland ice sheet: High-elevation balance and peripheral thinning, *Science*, *289*, 428–430, doi:10.1126/science.289.5478.428.

Kwok, R., and D. A. Rothrock (2009), Decline in Arctic sea ice thickness from submarine and ICESat records: 1958–2008, *Geophys. Res. Lett.*, *36*, L15501, doi:10.1029/2009GL039035.

Kwok, R., G. F. Cunningham, M. Wensnahan, I. Rigor, H. J. Zwally, and D. Yi (2009), Thinning and volume loss of the Arctic Ocean sea ice cover: 2003–2008, *J. Geophys. Res.*, *114*, C07005, doi:10.1029/2009JC005312.

Lauderdale, J. M., S. Bacon, A. C. N. Garabato, and N. P. Holliday (2008), Intensified turbulent mixing in the boundary current system of southern Greenland, *Geophys. Res. Lett.*, *35*, L04611, doi:10.1029/2007GL032785.

Laxon, S., N. Peacock, and D. Smith (2003), High interannual variability of sea ice thickness in the Arctic region, *Nature*, *425*, 947–950, doi:10.1038/nature02050.

Luckman, A., T. Murray, R. de Lange, and E. Hanna (2006), Rapid and synchronous ice-dynamic changes in East Greenland, *Geophys. Res. Lett.*, *33*, L03503, doi:10.1029/2005GL025428.

Macdonald, R. W., D. W. Paton, E. C. Carmack, and A. Omstedt (1995), The freshwater budget and under-ice spreading of Mackenzie River water in the Canadian Beaufort Sea based on salinity and $^{18}O/^{16}O$ measurements in water and ice, *J. Geophys. Res.*, *100*, 895–919, doi:10.1029/94JC02700.

McClelland, J. W., S. J. Déry, B. J. Peterson, R. M. Holmes, and E. F. Wood (2006), A pan-Arctic evaluation of changes in river discharge during the latter half of the 20th century, *Geophys. Res. Lett.*, *33*, L06715, doi:10.1029/2006GL025753.

McPhee, M. G., A. Proshutinsky, J. H. Morison, M. Steele, and M. B. Alkire (2009), Rapid change in freshwater content of the Arctic Ocean, *Geophys. Res. Lett.*, *36*, L10602, doi:10.1029/2009GL037525.

Meredith, M., K. Heywood, P. Dennis, L. Goldson, R. White, E. Fahrbach, U. Schauer, and S. Osterhus (2001), Freshwater fluxes through the western Fram Strait, *Geophys. Res. Lett.*, *28*, 1615–1618, doi:10.1029/2000GL011992.

Naveira Garabato, A. C. N., K. I. C. Oliver, A. J. Watson, and M. J. Messias (2004), Turbulent diapycnal mixing in the Nordic seas, *J. Geophys. Res.*, *109*, C12010, doi:10.1029/2004JC002411.

New, M., M. Todd, M. Hulme, and P. Jones (2001), Precipitation measurements and trends in the twentieth century, *Int. J. Clim.*, *21*, 1899–1922, doi:10.1002/joc.680.

Osterkamp, T. E. (2005), The recent waning of permafrost in Alaska, *Global Planet. Change*, *49*, 187–202, doi:10.1016/j.gloplacha.2005.09.001.

Osterkamp, T. E., and V. E. Romanovsky (1999), Evidence for warming and thawing of discontinuous permafrost in Alaska, *Permafrost Periglacial Processes*, *10*, 17–37, doi:10.1002/(SICI)1099-1530(199901/03)10:1<17::AID-PPP303>3.0.CO;2-4.

Östlund, H. G., and G. Hut (1984), Arctic Ocean water mass balance from isotope data, *J. Geophys. Res.*, *89*, 6373–6381, doi:10.1029/JC089iC04p06373.

Östlund, H. G., H. Craig, W. S. Broecker, and D. Spenser (1987), *GEOSECS Atlantic, Pacific Shorebased Data and Graphics and Indian Ocean Expeditions*, vol. 7, Natl. Sci. Found., Washington, D. C.

Perovich, D. K., C. S. Roesler, and W. S. Pegau (1998), Variability in Arctic sea ice optical properties, *J. Geophys. Res.*, *103*, 1193–1208, doi:10.1029/97JC01614.

Peterson, B. J., R. M. Holmes, J. W. McClelland, C. J. Vorosmarty, R. B. Lammers, A. I. Shiklomanov, I. A. Shiklomanov, and S. Rahmstorf (2002), Increasing river discharge to the Arctic Ocean, *Science*, *298*, 2171–2173, doi:10.1126/science.1077445.

Peterson, B. J., J. McClelland, R. Curry, R. M. Holmes, J. E. Walsh, and K. Aagaard (2006), Trajectory shifts in the Arctic and subarctic freshwater cycle, *Science*, *313*, 1061–1066, doi:10.1126/science.1122593.

Pickart, R. S., D. J. Torres, and P. S. Fratantoni (2005), The east Greenland spill jet, *J. Phys. Oceanogr.*, *35*, 1037–1053, doi:10.1175/JPO2734.1.

Rabe, B., U. Schauer, A. Mackensen, M. Karcher, E. Hansen, and A. Beszczynska-Moller (2009), Freshwater components and transports in the Fram Strait—Recent observations and changes since the late 1990s, *Ocean Sci.*, *5*, 219–233, doi:10.5194/os-5-219-2009.

Reeh, N., H. Oerter, and H. H. Thomsen (2002), Comparison between Greenland ice-margin and ice-core oxygen-18 records, *Ann. Glaciol.*, *35*, 136–144.

Rignot, E., and P. Kanagaratnam (2006), Changes in the velocity structure of the Greenland ice sheet, *Science*, *311*, 986–990, doi:10.1126/science.1121381.

Rignot, E., and R. H. Thomas (2002), Mass balance of polar ice sheets, *Science*, *297*, 1502–1506, doi:10.1126/science.1073888.

Rignot, E., D. Braaten, S. P. Gogineni, W. B. Krabill, and J. R. McConnell (2004), Rapid ice discharge from southeast Greenland glaciers, *Geophys. Res. Lett.*, *31*, L10401, doi:10.1029/2004GL019474.

Rozanski, K., L. Araguas-Araguas, and R. Gonfiantini (1993), Isotopic patterns in modern global precipitation, in *Climate Change in Continental Isotopic Records, Geophys. Monogr. Ser.*, vol. 78, edited by P. K. Swart et al., pp. 1–37, AGU, Washington, D. C.

Schlichtholz, P., and M. N. Houssais (1999), An investigation of the dynamics of the East Greenland Current in Fram Strait based on a simple analytical model, *J. Phys. Oceanogr.*, *29*, 2240–2265, doi:10.1175/1520-0485(1999)029<2240:AIOTDO>2.0.CO;2.

Schmidt, G. A., G. R. Bigg, and E. J. Rohling (1999), Global Seawater Oxygen-18 Database, http://data.giss.nasa.gov/o18data/, Goddard Inst. for Space Stud., New York.

Shiklomanov, I. A., A. I. Shiklomanov, R. B. Lammers, B. J. Peterson, and C. J. Vorosmarty (2000), The dynamics of river water inflow to the Arctic Ocean, in *Freshwater Budget of the Arctic Ocean, NATO Sci. Partnership Sub-Ser.*, vol. 2, *Environ. Secur. Ser.*, vol. 70, edited by E. L. Lewis et al., pp. 281–296, Kluwer Acad., Dordrecht, Netherlands.

Solomon, S., D. Qin, M. Manning, Z. Chen, M. Marquis, K. B. Averyt, M. Tignor, and H. L. Miller (Eds.) (2007), *Climate Change 2007: The Physical Basis: Working Group I Contribution to the Fourth Assessment Report of the IPCC*, Cambridge Univ. Press, New York.

Spreen, G., S. Kern, D. Stammer, and E. Hansen (2009), Fram Strait sea ice volume export estimated between 2003 and 2008 from satellite data, *Geophys. Res. Lett.*, *36*, L19502, doi:10.1029/2009GL039591.

Stouffer, R. J., et al. (2006), Investigating the causes of the response of the thermohaline circulation to past and future climate changes, *J. Clim.*, *19*, 1365–1387, doi:10.1175/JCLI3689.1.

Stroeve, J. C., M. C. Serreze, F. Fetterer, T. Arbetter, W. Meier, J. Maslanik, and K. Knowles (2005), Tracking the Arctic's shrinking ice cover: Another extreme September minimum in 2004, *Geophys. Res. Lett.*, *32*, L04501, doi:10.1029/2004GL021810.

Stroeve, J., M. M. Holland, W. Meier, T. Scambos, and M. Serreze (2007), Arctic sea ice decline: Faster than forecast, *Geophys. Res. Lett.*, *34*, L09501, doi:10.1029/2007GL029703.

Sutherland, D. A., and C. Cenedese (2009), Laboratory experiments on the interaction of a buoyant coastal current with a canyon: Application to the East Greenland Current, *J. Phys. Oceanogr.*, *39*, 1258–1271, doi:10.1175/2008JPO4028.1.

Sutherland, D. A., and R. S. Pickart (2008), The East Greenland Coastal Current: Structure, variability, and forcing, *Prog. Oceanogr.*, *78*, 58–77, doi:10.1016/j.pocean.2007.09.006.

Sutherland, D. A., R. S. Pickart, E. P. Jones, K. Azetsu-Scott, A. J. Eert, and J. Olafsson (2009), Freshwater composition of the waters off southeast Greenland and their link to the Arctic Ocean, *J. Geophys. Res.*, *114*, C05020, doi:10.1029/2008JC004808.

Thomas, D., S. Martin, D. Rothrock, and M. Steele (1996), Assimilating satellite concentration data into an Arctic sea ice mass balance model, 1979–1985, *J. Geophys. Res.*, *101*, 20,849–20,868, doi:10.1029/96JC01690.

van den Broeke, M., J. Bamber, J. Ettema, E. Rignot, E. Schrama, W. J. van de Berg, E. van Meijgaard, I. Velicogna, and B. Wouters (2009), Partitioning recent Greenland mass loss, *Science*, *326*, 984–986, doi:10.1126/science.1178176.

Velicogna, I. (2009), Increasing rates of ice mass loss from the Greenland and Antarctic ice sheets revealed by GRACE, *Geophys. Res. Lett.*, *36*, L19503, doi:10.1029/2009GL040222.

Warren, S. G., I. G. Rigor, N. Untersteiner, V. F. Radionov, N. N. Bryazgin, Y. I. Aleksandrov, and R. Colony (1999), Snow depth on Arctic sea ice, *J. Clim.*, *12*, 1814–1829, doi:10.1175/1520-0442(1999)012<1814:SDOASI>2.0.CO;2.

Wilkinson, D., and S. Bacon (2005), The spatial and temporal variability of the East Greenland Coastal Current from historic data, *Geophys. Res. Lett.*, *32*, L24618, doi:10.1029/2005GL024232.

Winters, T. (1999), Oxygen isotope ratios in seawater of the North Atlantic, Ph.D. thesis, Sch. of Environ. Sci., Univ. of East Anglia, Norwich, U. K.

Wu, P. L., R. Wood, and P. Stott (2005), Human influence on increasing Arctic river discharges, *Geophys. Res. Lett.*, *32*, L02703, doi:10.1029/2004GL021570.

Yamamoto-Kawai, M., N. Tanaka, and S. Pivovarov (2005), Freshwater and brine behaviors in the Arctic Ocean deduced from historical data of δ^{18}O and alkalinity (1929–2002 A.D.), *J. Geophys. Res.*, *110*, C10003, doi:10.1029/2004JC002793.

Yamamoto-Kawai, M., F. A. McLaughlin, E. C. Carmack, S. Nishino, K. Shimada, and N. Kurita (2009), Surface freshening of the Canada Basin, 2003–2007: River runoff versus sea ice meltwater, *J. Geophys. Res.*, *114*, C00A05, doi:10.1029/2008JC005000.

S. Bacon, M. Bolshaw, K. A. Cox, E. J. Rohling, J. D. Stanford, and D. Wilkinson, National Oceanography Centre, Southampton, School of Ocean and Earth Science, University of Southampton, Waterfront Campus, European Way, Southampton SO14 3ZH, UK.

S. De la Rosa, Geophysical Institute, University of Bergen, Allégaten 70, N-5007 Bergen, Norway.

P. A. Dodd, Norsk Polarinstitutt, Polarmiljøsenteret, Hjalmar Johansens gate 14, N-9296 Tromsø, Norway.

K. J. Heywood, School of Environmental Sciences, University of East Anglia, Norwich NR4 7TJ, UK.

A. J. McVicar, Department of Earth Science and Engineering, Imperial College, South Kensington Campus, London SW7 2AZ, UK.